Project Report
ATC-255

ASR-9 Weather Systems Processor (WSP) Signal Processing Algorithms

M.E. Weber

25 June 2002

Lincoln Laboratory
MASSACHUSETTS INSTITUTE OF TECHNOLOGY
LEXINGTON, MASSACHUSETTS

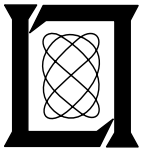

Prepared for the Federal Aviation Administration,
Washington, D.C. 20591

This document is available to the public through
the National Technical Information Service,
Springfield, VA 22161

This document is disseminated under the sponsorship of the Department of Transportation in the interest of information exchange. The United States Government assumes no liability for its contents or use thereof.

TECHNICAL REPORT STANDARD TITLE PAGE

1. Report No.	2. Government Accession No.	3. Recipient's Catalog No.
ATC-255		

4. Title and Subtitle	5. Report Date
ASR-9 Weather Systems Processor (WSP) Signal Processing Algorithms	25 June 2002
	6. Performing Organization Code

7. Author(s)	8. Performing Organization Report No.
Mark E. Weber	ATC-255

9. Performing Organization Name and Address	10. Work Unit No. (TRAIS)
MIT Lincoln Laboratory 244 Wood Street Lexington, MA 02420-9108	11. Contract or Grant No. F19628-00-C-0002

12. Sponsoring Agency Name and Address	13. Type of Report and Period Covered
Department of Transportation Federal Aviation Administration 800 Independence Ave., S.W. Washington, D.C. 20591	Project Report
	14. Sponsoring Agency Code

15. Supplementary Notes

This report is based on studies performed at Lincoln Laboratory, a center for research operated by Massachusetts Institute of Technology, under Air Force Contract F19628-00-C-0002.

16. Abstract

Thunderstorm activity and associated low-altitude wind shear constitute a significant safety hazard to aviation, particular during operations near airport terminals where aircraft altitude is low and flight routes are constrained. The Federal Aviation Administration (FAA) has procured several dedicated meteorological sensors (Terminal Doppler Weather Radar (TDWR), Network Expansion Low Level Wind Shear Alert System (LLWAS)) at major airports to enhance the safety and efficiency of operations during convective weather. A hardware and software modification to existing Airport Surveillance Radars (ASR-9)–the Weather Systems Processor (WSP)–will provide similar capabilities at much lower cost, thus allowing the FAA to extend its protection envelope to medium density airports and airports where thunderstorm activity is less frequent. Following successful operational demonstrations of a prototype ASR-WSP, the FAA has procured approximately 35 WSPs for nationwide deployment. Lincoln Laboratory was responsible for development of all data processing algorithms, which were provided as Government Furnished Equipment (GFE), to be implemented by the full-scale development (FSD) contractor without modification.

This report defines the operations that are used to produce images of atmospheric reflectivity, Doppler velocity and data quality that are used by WSP's meteorological product algorithms to generate automated information on hazardous wind shear and other phenomena. Principal requirements are suppression of interference (e.g., ground clutter, moving point targets, meteorological and ground echoes originating from beyond the radar's unambiguous range), generation of meteorologically relevant images and estimates of data quality. Hereafter, these operations will be referred to as "signal processing" and the resulting images as "base data."

17. Key Words	18. Distribution Statement
	This document is available to the public through the National Technical Information Service, Springfield, VA 22161.

19. Security Classif. (of this report)	20. Security Classif. (of this page)	21. No. of Pages	22. Price
Unclassified	Unclassified	63	

FORM DOT F 1700.7 (8-72) Reproduction of completed page authorized

ABSTRACT

Thunderstorm activity and associated low-altitude wind shear constitute a significant safety hazard to aviation, particular during operations near airport terminals where aircraft altitude is low and flight routes are constrained. The Federal Aviation Administration (FAA) has procured several dedicated meteorological sensors (Terminal Doppler Weather Radar (TDWR), Network Expansion Low Level Wind Shear Alert System (LLWAS)) at major airports to enhance the safety and efficiency of operations during convective weather. A hardware and software modification to existing Airport Surveillance Radars (ASR-9)–the Weather Systems Processor (WSP)–will provide similar capabilities at much lower cost, thus allowing the FAA to extend its protection envelope to medium density airports and airports where thunderstorm activity is less frequent. Following successful operational demonstrations of a prototype ASR-WSP, the FAA has procured approximately 35 WSPs for nationwide deployment. Lincoln Laboratory was responsible for development of all data processing algorithms, which were provided as Government Furnished Equipment (GFE), to be implemented by the full-scale development (FSD) contractor without modification.

This report defines the operations that are used to produce images of atmospheric reflectivity, Doppler velocity and data quality that are used by WSP's meteorological product algorithms to generate automated information on hazardous wind shear and other phenomena. Principal requirements are suppression of interference (e.g., ground clutter, moving point targets, meteorological and ground echoes originating from beyond the radar's unambiguous range), generation of meteorologically relevant images and estimates of data quality. Hereafter, these operations will be referred to as "signal processing" and the resulting images as "base data."

TABLE OF CONTENTS

TABLE OF CONTENTS
(Continued)

LIST OF ILLUSTRATIONS

LIST OF TABLES

1. INTRODUCTION

Thunderstorm activity and associated low-altitude wind shear constitute a significant safety hazard to aviation, particular during operations near airport terminals where aircraft altitude is low and flight routes are constrained. The Federal Aviation Administration (FAA) has procured several dedicated meteorological sensors (Terminal Doppler Weather Radar (TDWR), Network Expansion Low Level Wind Shear Alert System (LLWAS)) at major airports to enhance the safety and efficiency of operations during convective weather. A hardware and software modification to existing Airport Surveillance Radars (ASR-9)–the Weather Systems Processor (WSP)–will provide similar capabilities at much lower cost, thus allowing the FAA to extend its protection envelope to medium density airports and airports where thunderstorm activity is less frequent. Following successful operational demonstrations of a prototype ASR-WSP, the FAA has procured approximately 35 WSPs for nationwide deployment. Lincoln Laboratory was responsible for development of all data processing algorithms, which were provided as Government Furnished Equipment (GFE), to be implemented by the full-scale development (FSD) contractor without modification.

This report defines the operations that are used to produce images of atmospheric reflectivity, Doppler velocity and data quality that are used by WSP's meteorological product algorithms to generate automated information on hazardous wind shear and other phenomena. Principal requirements are suppression of interference (e.g., ground clutter, moving point targets, meteorological and ground echoes originating from beyond the radar's unambiguous range), generation of meteorologically relevant images and estimates of data quality. Hereafter, these operations will be referred to as "signal processing" and the resulting images as "base data." Signal processing operations are a major driver on the WSP's computation speed and memory requirements. Although exact figures depend on details of the implementation approach, we estimate that the algorithms defined in this report require a computer capable of accomplishing approximately 100 million floating point multiply/add operations per second (MFLOPS). Associated memory requirements are 50 million bytes (MBYTES). In contrast, signal processing software implementation is straightforward relative to many of the WSP's meteorological product algorithms; most operations are accomplished via well-defined arithmetic operations (e.g., vector-matrix multiply, vector dot product) applied identically to successive range-azimuth resolution cells.

The WSP's signal processing algorithms are severely constrained by the parameters of its host radar and its requirement to coexist transparently with the ASR-9 target channel. Major data processing issues are discussed in [1][2][3]. Reference [4] provides details on the ASR-9 and recommended hardware interfaces between the WSP and its host ASR-9. For completeness we list the major points of these reports here:

1. Suppression of ground clutter through the use of Finite Impulse Response (FIR) filters and subsequent estimation of base data requires coherent processing of more pulses than are

available from the individual constant-PRF pulse blocks transmitted by the ASR-9. WSP signal processing operations are performed using an "extended coherent processing interval" (hereafter abbreviated ECPI) that spans three successive constant-PRF blocks. The coherent processing operations must account for the resulting changes in PRF within this ECPI;

2. The FIR high pass filters used for ground clutter suppression are adaptively selected on a range-gate by gate basis–using clear day maps of associated clutter residue–in order to minimize possible biases in the base data estimates caused by distortion of the weather echo spectra;

3. The base data fields required by the meteorological product algorithms are generated from high and low beam data, acquired from antenna ports appropriate to the transmitter polarization mode (linear or circular). In contrast to the target channel's range-azimuth gated high and low beam acquisition and processing mode, the WSP must combine high/low beam signals that are acquired near simultaneously in the same range gate to generate necessary base data; and

4. Gate-to-gate and scan-to-scan filtering is required to eliminate moving point targets and ground clutter breakthrough from the base data fields, and to reduce Doppler moment estimate variance to acceptable levels.

The organization of this report is as follows. Section 2 summarizes relevant parameters of the ASR-9 and defines inputs to the WSP's signal processing algorithms. In Section 3, we define the base data fields that are output to the WSP's meteorological product generation algorithms. Definition of the signal processing operations is provided in Section 4, the largest portion of this report.

2. WSP INPUTS

2.1 RELEVANT ASR-9 PARAMETERS

The ASR-9 operates at a selectable frequency between 2.7 and 2.9 GHz. It transmits a 1.12 MW peak power, 1 μsec pulse at average pulse repetition frequencies (PRF) that vary from 1050 to 1200 pulses per second. During the time interval in which the ASR-9's antenna scans through one beamwidth in azimuth, it transmits two trains of pulses at pulse repetition intervals (PRI) that vary by the ratio of 9:7. Ten pulses are transmitted at the high pulse repetition frequency (PRF) followed by eight pulses at the low PRF; from 1 to 3 fill pulses at the low PRF may be inserted following the low PRF block in order to maintain scan-to-scan synchronization of the pulse transmissions with antenna azimuth under wind loading conditions. The ASR-9's target channel separately coherently processes the two pulse trains in order to mitigate aircraft blind speeds.

The radar's doubly curved reflector is scanned in azimuth at a rate of 75 degrees/second. Its azimuth half-power beamwidth is 1.4 degrees and its elevation beamwidth is 4.8 degrees with an approximately cosecant squared falloff above the nose of the beam. Processing space is divided into 256 azimuth "sectors," each 1.4° in extent, and 960 range gates, each 111 m (1/16 nmi) in extent. As mentioned, pulse transmission is synchronized with antenna rotation so that the radar resolution cells defined by coherent processing operations are precisely collocated from scan to scan. This supports the utilization of fine-grain maps for storage of *a priori* information on stationary ground clutter, roadways and other interference sources.

"High" and "low" antenna patterns are employed by the target channel in a range-azimuth gated (RAG) mode to reduce interference from ground clutter at short range, while maintaining low altitude surveillance at longer ranges. Typically, the target channel switches its input from the high to the low receiving beam at a range of 15 nmi. Figure 1 plots the elevation gain patterns of the ASR-9. Pulse transmission occurs through the feed horn associated with the low antenna pattern. Two way gain patterns are therefore the product of the low beam pattern and the pattern of the beam (high or low) used for signal reception.

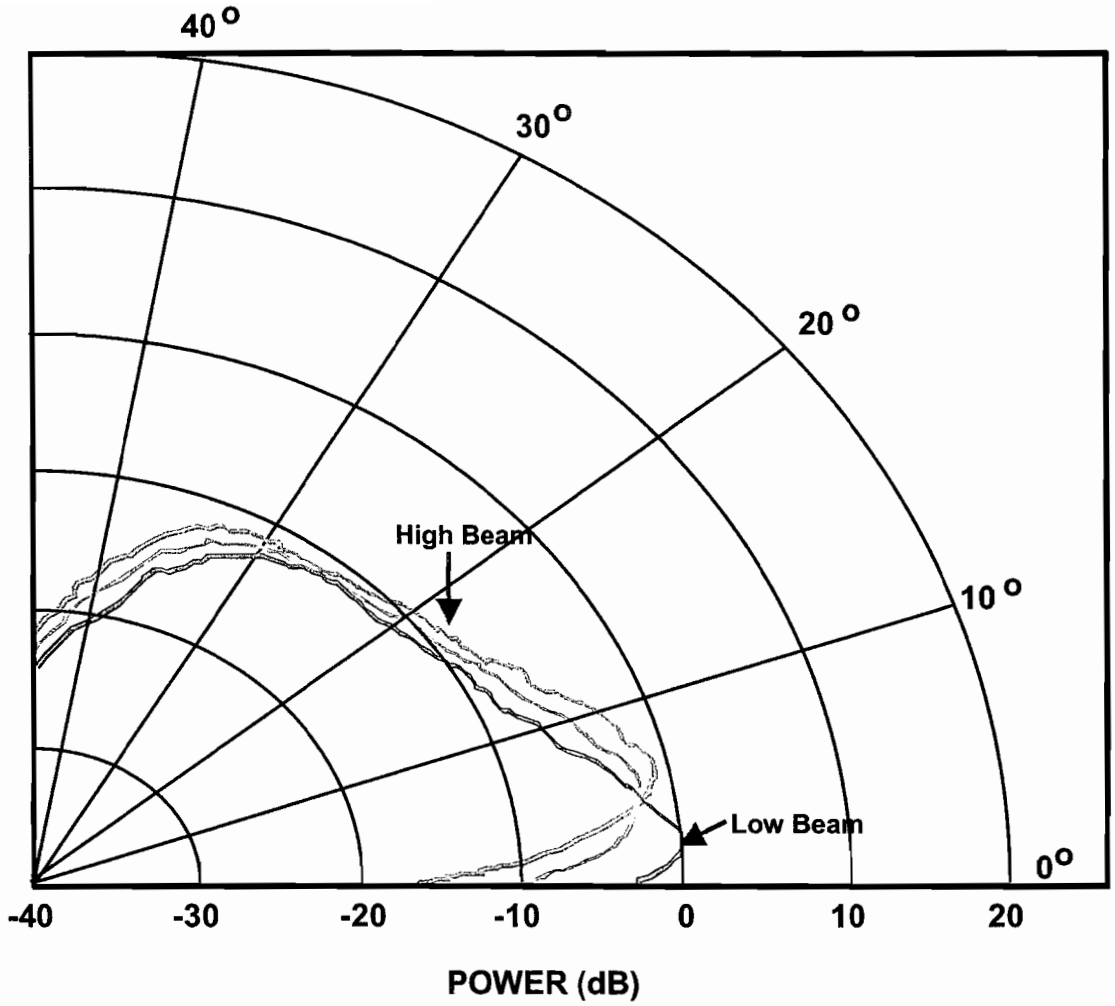

Figure 1. ASR-9 one-way elevation beam patterns. The blue line is the effective high beam pattern given that signal transmission is through the low beam.

The ASR-9 can transmit either vertical linearly polarized (LP) signals or Right Hand Sense circularly polarized (CP) signals. The former is the default but the radar will automatically switch to circularly polarized transmission when significant precipitation exists within its coverage area. The antenna feeds have separate receive ports for both "co-polarized" and "cross-polarized" signals. In LP transmission mode, the co-polarized ports receive vertically polarized echoes and cross-polarized receive horizontally polarized returns. (Obviously there is negligible energy in the cross-polarized signal in this mode). In CP mode, the co- and cross-polarized ports receive respectively the right- and left-hand-sense circularly polarized signals. The latter is appropriate for processing of returns from precipitation since most of the energy scattered from spherical hydrometeors is returned with opposite sense circular polarization. The aircraft target channel continues to process co-polarized signals since precipitation clutter is reduced

substantially (10-15 dB) whereas returns from a complex aircraft target are typically equally split between the two polarizations (i.e., 3 dB down in each channel).

2.2 WSP SIGNAL PROCESSOR INPUTS

2.2.1 RF Signal Paths

Data signals input to the WSP signal processing computer from the ASR-9 consist of:

- Quadrature video samples from a receive chain installed specifically for the WSP; and
- Simultaneous quadrature samples from the active target channel analog/digital (A/D) converters.

Signals acquired through the dedicated WSP receive chain have significantly larger dynamic range and minimum detectable signal level than those processed through the target channel receiver. These are the primary source for the Doppler imagery that is used in detection of low altitude wind shear phenomena. Target channel A/D output is used for developing weather reflectivity images where all necessary signals are not derivable from the WSP receive chain. As discussed in [4], the signals feeding the WSP's dedicated receive chain are derived through a network of RF switches and couplers. Since the details of the WSP to ASR-9 interfaces are closely coupled its signal processing operations, we will discuss the radar signal paths in detail.

Figure 2 diagrams RF signal paths for the WSP signal processor inputs. The inputs to the WSP signal processing computer are a function of the "state" of the radar. In this context, "state" refers to the ASR-9's transmit polarization, the target channel's RAG beam control selection (governing switches "A" and "B" in Figure 2) and the setting of the WSP-controlled beam switches ("C" through "E" in Figure 2) which control "even scan" (low beam) or "odd scan" (high beam) data collection for the WSP receive chain. Table 1 defines the WSP's inputs as a function of radar state. All states must be accommodated by the WSP computers.

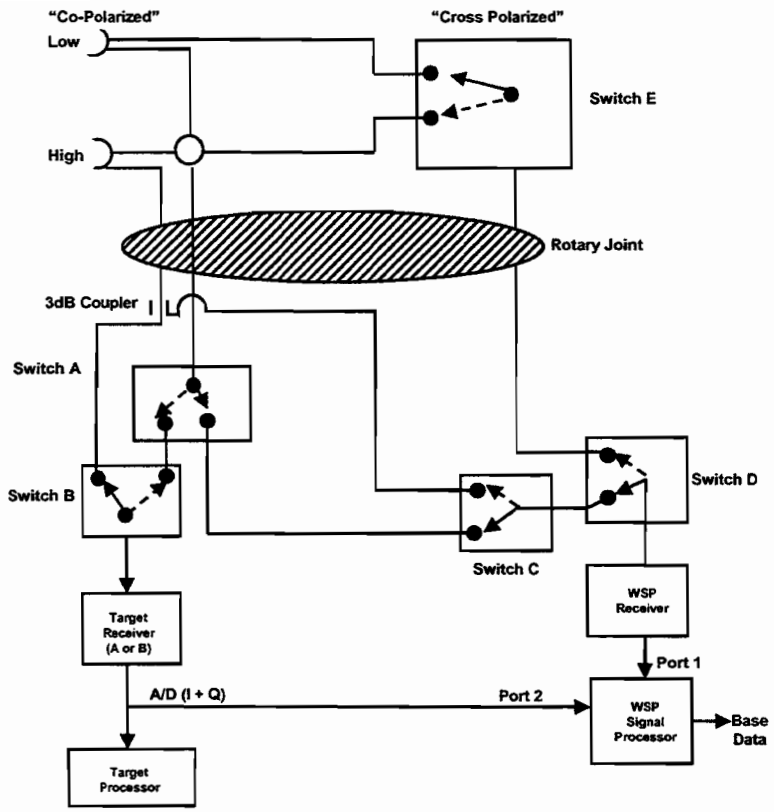

Figure 2. RF Signal paths to the WSP signal processor inputs. This simplified diagram does not show additional paths and switches necessary to support the ASR-9's dual-redundant transmit/receive architecture.

TABLE 1

RF Signal Inputs to WSP Signal Processor Computer

	Linear Polarization				Circular Polarization			
	Even Scans		Odd Scans		Even Scans		Odd Scans	
Target Chan. RAG	**High <15nmi**	**Low >15nmi**	**High <15nmi**	**Low >15nmi**	**High <15nmi**	**Low >15nmi**	**High <15nmi**	**Low >15nmi**
Port 1 (WSP Rx)	Low Co-Pol	No Input	High Co-Pol	High Co-Pol	Low Cross-Pol	Low Cross-Pol	High Cross-Pol	High Cross-Pol
Port 2 (Target Rx)	High Co-Pol	Low Co-Pol	High Co-Pol	Low Co-Pol	High Co-Pol	Low Co-Pol	High Co-Pol	Low Co-Pol

When the ASR-9 is in LP transmission mode, the WSP's receive chain "shares" the co-polarized signals with the target channel. At short range (nominally 15 nmi or less) the RF switch labeled "B" in Figure 2 is set by the ASR-9's RAG control to shunt the high-beam signal to the active target channel. Under ASR-9 RAG control, switch "B" changes state at a programmable range (nominally 15 nmi) so that the low beam signal is input to the target channel at greater range. This beam switching mode for the target channel is a function only of the RAG control program (i.e. it is independent of transmit polarization and is the same on each antenna scan).

For all range gates within the short range interval of operational concern for wind shear detection (< 15 nmi), beam switches "A," "C," and "D" provide, on an alternating[1] scan basis, both low and high beam signals to the wide dynamic range WSP receive chain. Low beam signals are derived from beam switch "A" and are available only for the range interval where the target processor is connected to the high beam via switch "B". On "even" antenna scans, no signals are input to the WSP receive chain at ranges where the ASR-9 RAG program connects low beam signals to the target processor. On "odd" antenna scans, switch "C" connects the WSP receive chain to the co-polarized high beam signal, derived through a 3 dB coupler inserted in the high beam target channel receive path. The high beam signal is available to the WSP receive chain independent of target channel RAG selection.

---

[1] As explained below, these switches change state with a period somewhat greater than the antenna revolution period in order to avoid continual data degradation at a single azimuth from "switching transients."

When the ASR-9 is in CP transmission mode, precipitation returns will normally be almost entirely cross-polarized. In this mode, the WSP receive chain is connected through switch "D" to a single-pole double throw switch "E" above the ASR-9's rotary joint. Switch "E" feeds low and high beam cross-polarized signals to the WSP receive chain on an alternating basis (see again footnote 2). Under conditions of signal propagation along long paths of heavy rain or wet snow, depolarization in the returned signal may occur. The availability of co-polarized signals from the target channel A/D converters allows, in principle, for correction of reflectivity biases that might result in this scenario.

2.2.2 Alternate Scan Processing

Switches C or E in Figure 2 are used to switch the input to the high-dynamic range WSP receiver between high and low beams on an alternating basis. Switch C, used during LP transmission mode, is relatively slow and will prevent acquisition of WSP signals during at least one extended coherent processing interval (ECPI) while it changes position. Switch E, which is used during CP transmission mode, is an existing ASR-9 RAG switch and can change state in microseconds. However, because the WSP's ECPIs (see 2.2.3) overlap, the transition between high and low beam signals necessarily prevents processing of data from at least one ECPI at the switchover azimuth.

In either polarization, the signal processing computer ignores data from affected ECPIs and interpolates base data into the associated resolution cells through the use of spatial and scan to scan filters. To avoid introduction of a "dim azimuth" where missing data must be continuously interpolated, the switch azimuth between high and low beams must precess from scan to scan around the compass. The simplest algorithm for accomplishing this is for the switch azimuth to increase by a constant number of azimuth sectors on each antenna resolution. Straightforward calculations demonstrate that an increment of 75 sectors per scan (105.5° azimuth) maximizes the "separation" of switch azimuths. Here, "separation" is defined as the average product of switch azimuth separation times switch time separation; the averaging is performed over all pairs of beam transitions accomplished during the 256 scan period required for the whole cycle to repeat.

To illustrate, Table 2 defines the beam-switch progression for the first six and last three cycles in the progression.

TABLE 2

Beam Switching Progression for WSP Controlled Waveguide Switches

"Scan"	Start Sector (and Azimuth)	Stop Sector	Sectors Processed	Beam Switch Position
0	0 (0.0)	74	0-255 0-74	Low
1	75 (105.5)	149	75-255 0-149	High
2	150 (210.9)	224	150-255 0-224	Low
3	225 (316.4)	43	225-255 0-255 0-43	High
4	44 (61.9)	118	44-255 0-118	Low
5	119 (167.3)	193	119-255 0-193	High
---	---	---	---	---
253	31 (43.6)	105	31-255 0-105	High
254	106(149.1)	180	106-255 0-180	Low
255	181(254.5)	255	181-255 0-255	High

Note that throughout this beam switching sequence, the signal processing computer simply processes all range gates for each ECPI as it is clocked in, and writes the output of its autocorrelators (see Section 4) into the appropriate location [range, azimuth, high/low beam] in a "lags" memory buffer. Here the autocorrelation "lags" are recursively averaged with lags collected on previous antenna scans. Full base data images are output from the signal processor once per antenna scan, generated as described in Section 4 from the values currently stored in the "lags" buffer.

2.2.3 WSP Extended Coherent Processing Interval (ECPI)

Suppression of ground clutter and fine-resolution of Doppler velocity for low-altitude wind shear detection requires that coherent processing operations extend beyond the short (eight or ten) pulse blocks transmitted at constant PRF by the ASR-9. Examination of Figure 3 indicates that–given the indeterminate number of fill-pulses that will be inserted–a maximum of 27 pulses can be input to the WSP signal processor with known interpulse spacings. These extended Coherent Processing Interval (CPI's) (ECPI) are generated by:

1. Locating the first pulse in an azimuth sector, that is the first pulse of the ASR-9's high-PRF 10-pulse block;
2. Backing up eight pulses to select the first pulse of the WSP's ECPI; and
3. Reading this pulse and the following 26 pulses into memory for subsequent batch processing.

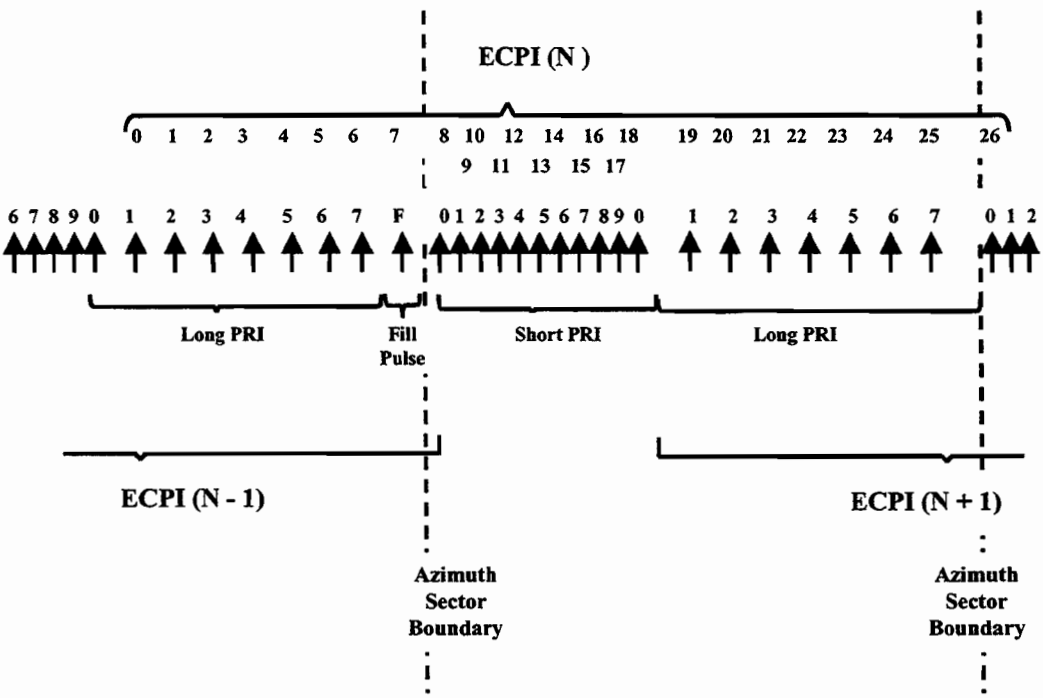

Figure 3. ASR-9 block staggered pulse transmission and their grouping for WSP into extended coherent processing intervals (ECPI).

Example ECPI's are illustrated in Figure 3. Note that within an ECPI, pulses 0-7 are derived from the low PRF CPI (and fill pulses if transmitted) of the preceding ASR-9 sector, pulses 8 through 25 correspond to the high and low PRF CPIs of the current ASR-9 sector, and pulse 26 is either a fill pulse for the current ASR-9 sector or is the first pulse of the succeeding sector's high PRF CPI. Whether or not a fill pulse is inserted after pulse 25, the PRI between pulses 25 and 26 will correspond to the low PRI.

Overlapping ECPIs are processed, one per sector, so as to output base data estimates for each of the 256 azimuth sectors processed by the ASR-9 target. For display purposes and algorithmic utilization the azimuth assigned to the base data corresponds to the center of the ECPI (that is, the azimuth of pulse #13).

2.2.4 Quadrature Sample Normalization

Quadrature samples input from both the WSP wide dynamic range receiver and the ASR-9's target channel receiver may be subject to range- and/or azimuth-dependent attenuation due to static Sensitivity Time Control (STC). Information necessary to correct sample amplitudes for these attenuators are input to the signal processor through access to associated ASR-9 and WSP Variable Site Parameters (VSPs).

2.2.5 Azimuth Reference and ECPI Timing

The ASR-9 outputs 4096 Azimuth Control Pulses (ACP) per revolution, along with one Azimuth Reference Pulse (ARP) at North. These are sampled and are transmitted to the WSP's signal processing computer in the header accompanying each transmitted pulse's 960-gate quadrature sample vector (hereafter referred to as "pulse header"). In addition, a 10.35 MHz clock internal to the ASR-9 is used to derive a "fast time" reference which is also included in this pulse header, thereby allowing the signal processor to deduce the pulse repetition interval between transmitted pulses.

Referring to Figure 3, it is clear that an unambiguous determination that a "sector crossing" has occurred can be accomplished by noting the PRI decrease at the beginning of the 10-pulse high PRF block. This transition is the primary means by which the signal processor blocks the incoming pulse stream into ECPIs. ACPs and ARPs are used for maintaining absolute azimuth registration and for recovery in the event of a loss of data.

2.2.6 Clock Time

A satellite clock provides reference time to the WSP signal processor. The signal processor assigns clock time explicitly to each archived base data field or quadrature sample vector.

2.2.7 Radar State

The pulse header includes full information on the ASR-9's "state" as defined in 2.2.1 (i.e., polarization, "odd" / "even" scan, ASR-9 RAG selection). This information defines the source of the quadrature samples according to Table 1.

3. SIGNAL PROCESSOR OUTPUTS

3.1 SUMMARY OF OUTPUT BASE DATA FIELDS

Table 3 summarizes the set of base data fields that are output from the WSP's signal processor. The columns list:

1. The name of the field;
2. The abbreviation that will be used for subsequent discussion;
3. The range interval and set of range gates for which the product is calculated;
4. Associated range resolution for each range interval; and
5. Which product generation algorithms make use of the base data field.

Base data are output in a polar coordinate system with the range resolutions indicated in Table 3 and angular resolution equal to one azimuth sector (1.4°). The signal processor outputs a complete set of base data once each antenna scan.

TABLE 3

Summary of Base Data Fields Output by WSP

Field Description	Abbreviation	Range (nmi)/Gates	Range Solution	Product Usage
Low Beam Reflectivity	LBDZ	0-15 / 1-240 16-60 / 241-420	1/16 nmi 1/4 nmi	gust front microburst
High Beam Reflectivity	HBDZ	0-15 / 1-240 16-60 / 241-420	1/16 nmi 1/4 nmi	gust front microburst
Dual Beam Reflectivity	DBDZ	0-15 / 1-240 16-60 / 241-420	1/16 nmi 1/4 nmi	gust front microburst precipitation storm motion
Low Beam Velocity	LBV	0-15 / 1-240 16-60 / 241-420	1/16 nmi 1/4 nmi	microburst gust front precipitation
High Beam Velocity	HBV	0-15 / 1-240 16-60 / 241-420	1/16 nmi 1/4 nmi	microburst precipitation
Dual Beam Velocity	DBV	0-15 / 1-240 16-60 / 241-420	1/16 nmi 1/4 nmi	microburst gust front
Low Beam Filter Selection	LBF	0-15 / 1-240 16-60 / 241-420	1/16 nmi 1/4 nmi	microburst gust front precipitation
High Beam Filter Selection	HBF	0-15 / 1-240 16-60 / 241-420	1/16 nmi 1/4 nmi	microburst gust front precipitation
Data Quality Flags	FLAGS	0-15 / 1-240 16-60 / 241-420	1/16 nmi 1/4 nmi	microburst gust front precipitation

3.2 BASE DATA FIELDS DESCRIPTIONS

3.2.1 Low-Beam Reflectivity (LBDZ)

Low Beam Reflectivity (LBDZ) is an estimate of the precipitation equivalent reflectivity factor (in dBz) measured by the ASR-9's low beam. LBDZ's primary application is for detection of gust front thin lines. Relative to surrounding clear air, atmospheric reflectivity is typically enhanced by the concentration of insects and other particulates in the converging winds at a gust front's leading edge. The relative amplitude of LBDZ and HBDZ are also used by the microburst detection algorithm in identifying reflectivity structures likely to be associated with false divergence signatures. The gust front detection algorithm likewise compares LBDZ and HBDZ to discriminate between true low altitude gust fronts and false-alarms caused by wind-borne, upper altitude cloud features such as "cloud streets."

3.2.2 High-Beam Reflectivity (HBDZ)

High-Beam Reflectivity (HBDZ) is an estimate of the precipitation equivalent reflectivity factor measured by the ASR-9's high beam. It is generated using only the output of the WSP receive chain. As noted above, HBDZ and LBDZ are compared to suppress microburst and gust front false alarms.

3.2.3 Dual Beam Reflectivity (DBDZ)

Dual Beam Reflectivity (DBDZ) is generated through combination of reflectivity estimates generated by the high and low receiving beams. It is generated as a (range-dependent) linear combination of high and low beam reflectivity estimates. The combining weight is a VSP and is by default set to provide high beam data to a range of 4km and low beam data at greater ranges. Low-beam signals used for DBDZ are derived from both the WSP receiving chain and the target channel A/D converters. As shown in Table 2, during LP transmission mode low beam signals are not available to the WSP receive chain at ranges beyond the 15 nmi nominal cutoff of the target channel high beam RAG window. Low beam data at greater ranges must be derived from the target channel A/D converters. High beam data are available through the WSP receiving chain at all ranges.

During CP transmission mode, both low- and high-beam cross-polarized returns are available at all ranges through the WSP receiving chain. Target channel low beam co-polarized returns, available at ranges beyond 15 nmi, could be used to correct for "depolarization bias" in the reflectivity estimates that may occur during CP transmission through heavy rain or wet hail. This capability is not, however, currently implemented in the WSP software.

The WSP's operational displays of six-level weather reflectivity are generated by thresholding of the DBDZ field at suitable levels, followed by additional spatial and scan-to-scan smoothing. This base data field is also the input to the WSP's storm motion and storm extrapolated position algorithms.

3.2.4 Low-Beam Velocity (LBV)

LBV is a "pulse-pair" estimate of the mean Doppler velocity of precipitation echoes received in the ASR-9's low receiving beam. In CP transmission mode, LBV is generated using signals from the WSP's receiving chain at all ranges. In LP transmission mode, low beam WSP receiving chain signals are available only to the 15 nmi range cutoff of the target channel RAG window; at greater ranges, the WSP utilizes target channel A/D output.

LBV is utilized by the gust front algorithm for detection of "velocity" thin lines. These are manifest in LBV images as moving lines of spatially coherent velocity estimates, embedded in a background of noise and (often) more slowly moving storm cells. The microburst detection algorithm also utilizes LBV and HBV in assessing the likelihood that divergence signatures correspond to true microbursts.

3.2.5 High-Beam Velocity (HBV)

High-Beam Velocity (HBV) is a "pulse-pair" estimate of the mean Doppler velocity of precipitation echoes received in the ASR-9's high receiving beam. In both CP and LP transmission mode, HBV is generated using signals from the WSP's receiving chain. It is used by the gust front algorithm for detection of velocity thin lines at short ranges where beam blockage or ground clutter interference may prevent usage of Low-Beam Velocity (LBV).

3.2.6 Dual-Beam Velocity (DBV)

Dual-Beam Velocity (DBV) is generated through combination of autocorrelation lags calculated for the low and high receiving beams. This combination exploits differences in the elevation gain patterns of the ASR's receive beams–specifically, the much greater gain of the low beam at near-horizon elevation angles (see Figure 1)–to "synthesize" a narrow response pattern to precipitation echoes near the horizon. This response pattern is necessary for accurate measurement of microburst outflow winds which occur in a very shallow layer near the surface. DBV is generated using only the output of the WSP receive chain.

3.2.7 Low beam Filter (LBF)

LBF encodes which of four clutter filters was selected for low beam processing for each range-azimuth resolution cell. LBF is used by the product generation algorithms in flagging data of low quality.

3.2.8 High Beam Filter (HBF)

HBF encodes which of four clutter filters was selected for high beam processing for each range-azimuth resolution cell.

3.2.9 Data Quality Flags (FLAGS)

The FLAGS field encodes individually the presence of conditions potentially affecting the validity of the base data estimates. The following conditions are flagged:

1. Ground clutter breakthrough caused by anomalous propagation (AP) (AP_FLAG);
2. Low signal-to-ground clutter residue (FILT_FAIL);
3. Out-of-trip weather contamination (OUT_OF_TRIP);
4. High local spatial variance in the LBV velocity field, indicative of low signal-to-noise and/or out-of-trip weather (VARIANCE).

4. SIGNAL PROCESSING ALGORITHMS

4.1 OVERVIEW

Figure 4 is an overview of the operations performed to compute base data from the quadrature video samples input to the two receiving ports of the WSP signal processor. These operations are performed independently for each range gate within each ECPI.

For each range gate within an ECPI, the radar "state" (see 2.2.1) defines which input I and Q stream will be processed by the signal processor. Input quadrature samples are normalized to account for receive path gain, STC, and differences in A/D word size between the WSP receive path and that of the ASR-9 target channel.

Ground clutter suppression is applied, utilizing static clutter residue maps of the site-specific ground clutter distribution to minimize distortions of the weather echo spectrum during the suppression process. The filtered echo samples are used to estimate the signal autocorrelation function at delays ("lags") of zero and one times the short and long-pulse PRIs transmitted by the ASR-9.

The autocorrelation lags are stored in a recursive-averaging buffer that smoothes the effects of the asynchronous, alternate-scan input of high and low beam data. Base data generation is performed once per antenna revolution based on the current values in this "lags buffer." Base data outputs and data quality flags are passed to the meteorological product generation algorithms.

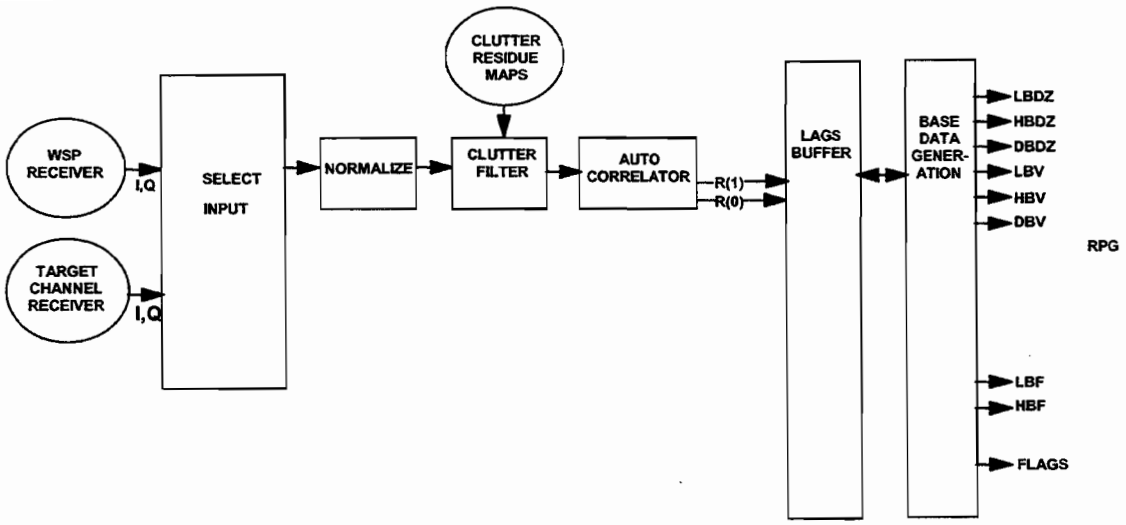

Figure 4. Overview of operations performed to compute base data from quadrature video samples input to the WSP signal processor.

4.2 PROCESSOR TIMING

All processing operations through storage of autocorrelation lags in the lags buffer shown in Figure 4 are accomplished once per ECPI for each range gate. The base data generation software modules access this buffer once per antenna revolution (nominally 4.8 seconds).

4.3 RANGE RESOLUTION

As indicated in Table 3, all products are generated with a range resolution equivalent to the A/D converter sampling rate (1/16 nmi) out to the 15 nmi limit for Doppler-based wind shear products. Base data required for generation of precipitation intensity maps and storm motion estimates at greater range are output with 1/4 nmi granularity. In this interval between 15 and 60 nmi, base data generation operations are performed on every fourth range gate.

4.4 VARIABLE SITE PARAMETERS

Variable Site Parameters (VSPs) control adaptation of the base data generation algorithms to the specific environmental and radar operating conditions of an individual site. Examples of VSPs are:

1. The four ground clutter filter transfer functions selected to span the range of suppression requirements for the clutter distribution at each site;

2. Clutter Residue Maps (CRM) that record the expected ground clutter residue power associated with each of the above four filter transfer functions. These are used in selecting the appropriate clutter filter for each range-azimuth bin from the four available. The Clutter Residue Maps (CRMs) assure that the filter selected adequately suppresses the clutter without unnecessarily distorting the weather Doppler spectrum;

3. The range dependent weighting coefficients for combination of low- and high-beam power measurements into the DBDZ reflectivity image used for operational display of storm intensity location and storm motion estimation;

4. The range-dependent beam weighting coefficient for combination of low and high beam autocorrelation lags for the DBV low altitude velocity estimate. Values for this weight are a function of the ASR-9 antenna elevation tilt and the expected depth of microburst outflows.

4.5 SIGNAL PROCESSING OPERATIONS

The following paragraphs define the operations required to process quadrature video samples into the base data images defined in Table 3. These operations are performed for each "valid" range gate of each ECPI. A "valid" ECPI is one where no pulse samples are subject to data loss or contamination caused by the beam switching circuits of either the ASR-9 (i.e., the RAG high-low beam switch) or the WSP (i.e., the switches that control alternate scan data collection). The WSP signal processor does not process data or update its "lags buffer" (Figure 4) for range gates that are not valid.

Note that operations performed on the radar input are essentially identical through the update of the "lags buffer," irrespective of whether input is from the high or low receiving beam.

4.5.1 Selection of Input

Where available, base data are derived from the WSP receiving chain whose wide dynamic range is most appropriate for measurement of wind shear phenomena. The exception to this last statement is during LP transmission mode where the WSP receive chain's access to necessary low beam signals is cut off at ranges beyond the (nominally 15 nmi) target channel RAG switch. In this circumstance, low beam input to the WSP signal processor is from the target channel A/D converters.

4.5.2 Sample Normalization and Floating Point Conversion

Input quadrature samples are normalized to account for applied STC, differences in receive path gain between channels and differences in A/D word size between the WSP receive path and that of the ASR-9 target channel. Determination of appropriate normalization factors requires a combination of:

1. Compile-time signal processing software variables, for example, to account for A/D word size variation;

2. Variable site parameters such as STC functions;

3. Remote Monitoring System (RMS) dynamic measurements of WSP and target channel receive path gain;

Normalization is accomplished on a per-sample basis. Normalized samples are converted to 32-bit floating point format for input to the clutter suppression module.

4.5.3 Clutter Suppression

Clutter Filter Implementation

High pass filters used to suppress returns from stationary ground targets are implemented as shift-variant linear operators applied successively to each of the 27 pulse samples in an ECPI. Mathematically, this operation is accomplished via multiplication of the 27-sample data vector by a 27x27 real element "filter matrix" H. In matrix notation, the filter output vector Y is related to the input data vector X by:

$$Y = H X \tag{1}$$

In practice, the achieved magnitude and phase response for the first and last filter output samples may exhibit significant degradation owing to effects analogous to those encountered when conventional Finite Impulse Response (FIR) filters run beyond available data samples. For this reason, subsequent coherent processing operations for the high-pass filter outputs utilize only samples 1 through 25 of the ECPI.

Readers are referred to reference [6] for theWSP filter design equations.

Filter Bank

Quadrature samples are processed through one of four clutter filters, selected according to the relative intensities of clutter, weather and system noise in each radar resolution cell. These filters realize (trivially) an all-pass transfer function ("Filter 0") and three high pass functions ("Filters 1" through "3") that achieve increasing levels of clutter suppression through increasingly broad and deep transition- and

stop-bands. The three high-pass filter suppression levels may be selected from a set of twelve, in accordance with the ground clutter distribution at a specific site. Appendix A plots the set of available filter transfer functions and describes an objective approach to choosing the three filters to be used at a site.

Filter Selection

One of the four filters is chosen for each range-azimuth resolution cell using an algorithm designed to minimize excessive filtering and associated distortion of weather echo spectrum content.

Selection Algorithm

As depicted in Figure 5, this algorithm utilizes Clutter Residue Maps (CRM). Generated under precipitation-free conditions, these maps encode–for each range azimuth resolution cell–the median intensity of low beam ground clutter residue for each filter. The filter selection algorithm "decision parameter" is the ratio of filter output power "Z_n" to corresponding CRM median clutter residue "R_n." The expectation value of this ratio is:

$$\text{(2)} \qquad \langle Zn / Rn \rangle = \left\langle \frac{\text{Precipitation Echo Power} + \text{Clutter Residue}}{\text{Clutter Residue}} \right\rangle$$

$$= \frac{\langle \text{Precipitation Echo Power} \rangle}{\langle \text{Clutter Residue} \rangle} + 1$$

When this ratio exceeds an appropriate threshold (designated "T_1"), we assume that weather base data estimates can be generated without significant bias from the ground clutter residue. As described in [2], a default setting of 12.6 (11 dB) is chosen for the VSP "T_1" to account for single-scan variability in actual ground clutter intensity relative to the "average" value stored in the CRMs.

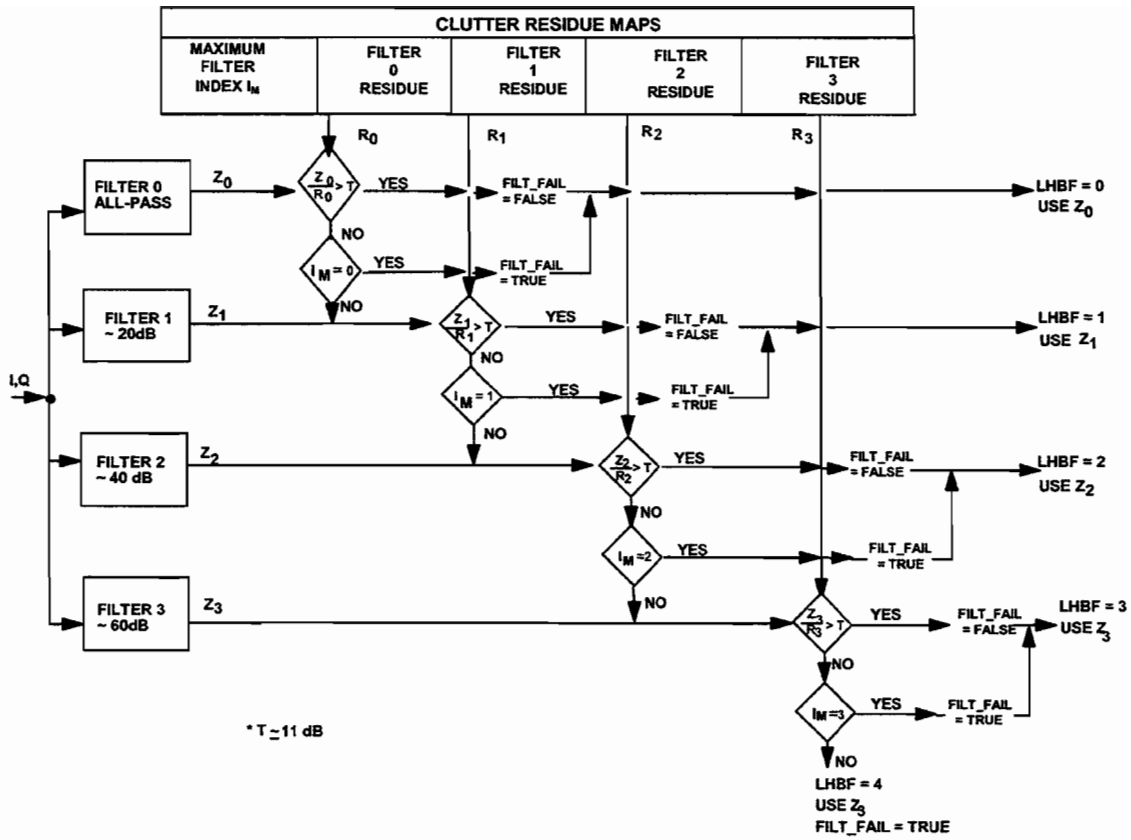

Figure 5. Filter selection algorithm's decision tree for selection of available clutter filters.

As shown in Figure 5, the filter selection algorithm tests this decision parameter for the available clutter filters in succession (0,1,2,3). The output of the first (i.e., least attenuating) filter which satisfies this test is selected for subsequent processing and its index is written into the corresponding filter selection LBF or HBF field. When the decision parameter test is satisfied for one of the four filters, a data quality flag FILT_FAIL is set to logical "False," indicating that a weather signal significantly exceeding clutter residue has been successfully detected.

Exception Conditions

Weather Signal Close to System Noise Floor: The CRMs also store the index ("I_M") of the least attenuating filter, which suppresses clutter residue below system noise. If the decision parameter test is not satisfied for this filter, we assume that weather power is sufficiently close to system noise that additional filtering will not improve its detectability relative to the net interference background (noise plus clutter residue). In this circumstance, the output of filter "I_M" is selected for subsequent processing.

Clutter Residue Exceeding both System Noise and Weather Signal: In the event that none of the available filters drive clutter residue below the system noise level and output weather power is not sufficient to satisfy the "decision parameter" test for any of the filters, the output of filter 3 is selected for subsequent processing, the index "4" is written to LBF or HBF and "FILT_FAIL" is set to "TRUE". These conditions inform subsequent meteorological product algorithms that clutter residue dominates system noise in this range gate, and that weather to clutter residue ratio is low (less than "T_1").

Clutter Residue Maps (CRM)

CRMs encode expected clutter residue power for each of the four clutter filters and each range-azimuth resolution cell within the WSP's instrumented range. In addition, the CRMs encode, for each range-azimuth resolution cell, the index of the least attenuating filter, which drives clutter residue power to the system noise level. CRMs are generated by the WSP in "off-line" mode by sampling weather-free returns over many successive antenna scans. Separate clutter maps are generated and used for the two polarization modes processed by the WSP:

1. Vertical linear polarization (transmit and receive);
2. Circular polarization. Cross-polarization receive.

Clutter Residue Estimation

For each available clutter filter (0 through 3), clutter residue is estimated on a precipitation-free day with normal propagation conditions by computing median filter output power over a minimum of 50 successive scans. To avoid excessive memory requirements for the CRM generation process, map generation is accomplished separately for each filter and incrementally over small azimuth intervals.

Maximum Filter Index

This index (I_M = 0,1,2, or 3) denotes the least attenuating filter, which drives the clutter residue level to or below the system noise level. Currently, I_M is set equal to one (corresponding to approximately 20 dB of clutter suppression) if the all-pass clutter power is within 18 dB of the noise floor. Otherwise it is set equal to three (corresponding to approximately 60 dB of suppression).

4.5.4 Autocorrelation

The signal autocorrelation function is estimated through straight-forward "dot product operations" applied to shifted versions of the sampled, filtered data vector. Hereafter, the autocorrelation function lags will be designated R(n), where n designates the number of pulse sample shifts that are applied prior to signal self-multiplication.

Calculation of Partial Autocorrelation Lag Estimates

Long- and short-PRI "partial" autocorrelation lag estimates are accumulated separately for the two pulse-pair separations encountered within an ECPI:

$$(3) \qquad R_{Long}(n) = \frac{1}{15-2n}\left\{\sum_{p=1}^{8-n} x_p x^*_{p+n} + \sum_{p=19}^{25-n} x_p x^*_{p+n}\right\}$$

$$R_{Short}(n) = \frac{1}{10-n}\sum_{p=9}^{18-n} x_p x^*_{p+n}$$

Here x_p represents the pth complex sample in the ECPI. Note that the pulse blocks that constitute these partial lag estimates are characterized by a constant PRI with respect to the pulse preceding each pulse processed. Echoes from the "second trip"–the primary source of out-of-trip returns–will fold into the same range gate for all pulses within $R_{Long}(n)$, and into a different range gate for all pulses within $R_{Short}(n)$.

The pulse blocks that constitute the partial lag estimates are also characterized by a constant PRI with respect to the pulse pairs processed. As a result, all pulse pairs within the partial lag R(1) estimates share a common unambiguous Doppler velocity.

Detection of Out of Trip Returns

When received signal power in a range gate is dominated by echoes emanating from within the unambiguous range associated with both PRIs, $R_{Short}(0)$ and $R_{Long}(0)$ have the same expected value. A statistically significant discrepancy between the two partial lag 0 estimates reflects out-of-trip contamination. The PRI affected by the out-of-trip scatterers will exhibit larger returned power than that receiving energy only from within its unambiguous range interval.

Detection of out-of-trip returns is accomplished by a threshold test on the magnitude of the ratio $R_{Short}(0) / R_{Long}(0)$. If:

$$(4) \qquad R_{Short}(0) / R_{Long}(0) > T_{out\_of\_trip}$$

the data quality flag "Out_of_Trip" is set "true" and the PRI to be used in subsequent processing, "PRI-Used", is set to "1" indicating that long-PRI data only will be used for subsequent processing. The threshold "$T_{out\_of\_trip}$" is nominally set to 7.0 (5 dB).

Conversely, if:

(5) $$R_{Short}(0) / R_{Long}(0) < 1 / T_{out\_of\_trip}$$

the flag "Out_of_Trip" is set "true" and the PRI to be used in subsequent processing, "PRI-Used", is set to "2" indicating that short-PRI data only will be used for subsequent processing.

If neither of the conditions (3) or (4) are encountered, "Out_of_Trip" is set "false" and "PRI_Used" is set to "0" indicating that data from both PRIs will be used in subsequent processing.

In practice, the index pri_used that is selected through these comparisons is smoothed using a running, six-scan consensus averager. This allows $T_{out\_of\_trip}$ to be set at a fairly low value, without inappropriately discarding one or other Pulse Repetition Frequency (PRF) block in the absence of range-ambiguous weather owing to statistical fluctuations in received power. A low value for $T_{out\_of\_trip}$ maximizes the probability that range-ambiguous returns will be detected and flagged.

Combination of Partial Autocorrelation Lag Estimates

Following detection of range folding conditions, the long- and short-PRI partial R(n) correlation estimates are combined as follows. If the range aliasing flag "Out_of_Trip" has been set "true," R(n) is computed from the appropriate partial autocorrelation lag estimate:

"Out_of_Trip" = "True"

(6) $$R(n) = R_{Long}(n) \qquad PRI\_Used = 1$$

$$R(n) = R_{Short}(n) \qquad PRI\_Used = 2$$

If echoes in both PRIs are dominated by first trip weather, R(n) is estimated by averaging the long- and short-PRI estimates:

"Out_of_Trip" = "False"

(7)
$$R(n) = \frac{15 - 2n}{25 - 3n} x\, R_{Long}(n) + \frac{10 - n}{25 - 3n} x\, R_{Short}(n)$$

The relative weightings of the two PRI's contributions are in proportion to the number of pulse-pairs they contribute. Note that this averaging of complex vectors–as opposed to phase angle, or equivalently mean Doppler velocity–finesses the potential issues associated with the different unambiguous velocities of the long- and short-PRI blocks. The phase angle of the combined R(1) vector is that which would be measured using a constant sampling interval equal to the value defined in Table 4 below.

Effective Autocorrelation Delays

The R(n) as calculated here involve pulse-pairs separated by differing intervals. They represent therefore, the autocorrelation function sampled at delays intermediate between multiples of the long and short PRIs transmitted by the ASR-9. Table 4 summarizes the effective autocorrelation sample delays, τ *(n),* as multiples of the short Pulse Repetition Interval (PRI) transmitted by the ASR-9. These average delays vary depending on which partial lag estimates are used in the final R(n) calculation, and on the value of "n".

TABLE 4

Effective Autocorrelation Sample Delays τ (n) in Multiples of ASR-9 Short PRI

	τ *(n)* / short PRI "PRI_Used" = 0	τ *(n)* / short PRI "PRI_Used" = 1	τ *(n)* / short PRI "PRI_Used" = 2
R(0)	0.0	0.0	0.0
R(1)	1.17	1.29	1.0
R(2)	2.33	2.57	2.0
R(3)	3.48	3.86	3.0

4.5.5 Lags Buffer

Autocorrelation lags are written to the "lags buffer" for asynchronous access by the base data generation modules. This memory contains elements for each 1/16 nmi by 1-ECPI resolution cell out to 16 nmi and for every fourth radar range gate thereafter. Its dimensionality is therefore 420 (range gates) x 256 (beams). The autocorrelation lags are averaged recursively with those from preceding scans. Thus, the memory elements in the lags buffer –RL(n) –are updated as:

(8) $$RL(n) = [1\text{-}b] \times RL(n) + b \times R(n)$$

where R(n) is the current scan autocorrelation estimate and b is the recursive averaging coefficient. The default setting for b is 0.5.

4.5.6 Base Data Generation

During each antenna scan, the lags buffer is accessed to generate the set of base data images defined in Table 3. The following paragraphs define the operations required for generating each base data element.

Low-Beam Reflectivity

(9) $$LBDZ = 10\log_{10}\left\{k\left[R_{Low}(0) - N_{Low}\right] range^2\right\}$$

where k is the "radar constant," comprised of factors defined, for example, in [5]. N_{Low} is the system noise in the low beam path expressed in units equivalent to those of $R_{Low}(0)$.

High Beam Reflectivity

(10) $$HBDZ = 10\log_{10}\left\{k\left[R_{High}(0) - N_{High}\right] range^2\right\}$$

Dual Beam Reflectivity (DBR)

(11) $$DBDZ = 10\log_{10}\left\{k\left[w_{Low}\left(R_{Low}(0) - N_{Low}\right) + w_{High}\left(R_{High}(0) - N_{High}\right)\right] range^2\right\}$$

The weighting coefficients, w_{Low} and w_{High} are functions of range and are site variable parameters.

Low-Beam Velocity (LBV)

This is the standard "pulse pair" mean Doppler velocity estimate.

(12)
$$LBV = \frac{C}{4\pi f \tau(1)\, PRI_{Short}} \phi\{R_{Low}(1)\}$$

where τ (1) is as defined in Table 4 and PRI_{Short} is the selected short-PRI in seconds.

High beam Velocity (HBV)

(13)
$$HBV = \frac{C}{4\pi f \tau(1)\, PRI_{Short}} \phi\{R_{High}(1)\}$$

Dual-Beam Velocity (DBV)

The considerations involved in generation of the DBV estimate of low-altitude radial velocity for microburst detection are discussed in [3]. The estimate for DBV is formed via the standard pulse-pair estimator applied to a weighted, linear sum of the measured high- and low-beam lag 1 autocorrelation samples:

(14)
$$DBV = \frac{C}{4\pi f \tau(1)\, PRI_{Short}} \phi\{R_{Low}(1) - Weight\, R_{High}(1)\}$$

where:

(15)
$$Weight = \frac{R_{Low}(0)\, x\, beam\_comb}{R_{High}(0)}$$

and the site adaptable parameter "beam_comb," a function of the ASR's antenna tilt angle, is typically set to 0.7 for the standard antenna tilt angle of 0°. (This setting places the nose of the ASR-9's low beam at 2.0° above the horizon.)

Data Quality Flags

With the exception of the flag for anomalous propagation-induced ground clutter (AP), generation of the data quality flags is either trivial or described elsewhere in this report.

Figure 6 shows how the outputs of the WSP clutter filter bank are used to detect anomalous propagation conditions. If the all-pass is selected, a check is made to determine whether the return significantly exceeds its normal intensity due to amplication of clutter by AP. This is accomplished by filtering the data with the least attenuating of the WSP clutter filters (the ~ 20 dB suppression filter) and evaluating the ratio of input to output power.

For stationary clutter signals with near-zero mean Doppler velocity and spectrum widths dominated by antenna scan modulation (0.72 m/s for the ASR-9), this ratio will of course approach 20 dB. Meteorological echoes often have non-zero mean Doppler velocities and almost always exhibit spectrum widths well in excess of the scan-modulation limit. Thus the filter input/output power ratio will be significantly lower. A threshold of 11 dB for this ratio has been found to reliably differentiate meteorological returns from ground clutter.

If the filter input/output power ratio is less than this threshold, processing proceeds with the unfiltered data. Otherwise, the data for this resolution cell are flagged as "AP contaminated". As shown, an attempt is made to recover potential weather returns underlying the intensified clutter by filtering the signals with the more strongly attenuating "filter 3".

If the initial filter selection algorithm does not detect all-pass power significantly in excess of its normal level, no check for AP-induced clutter intensification is invoked. The selection algorithm proceeds to successively evaluate the output of the three high-pass filters relative to their associated residue maps as described previously.

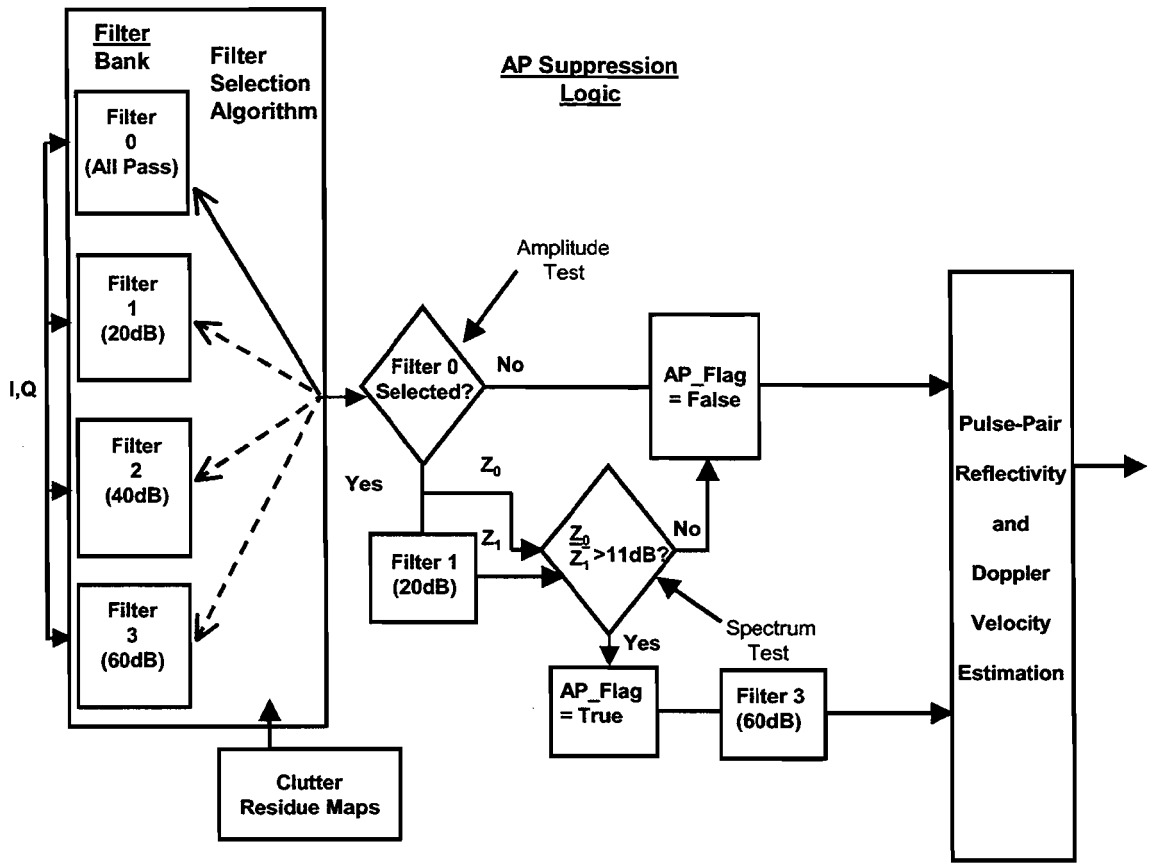

Figure 6. Flagging of ground clutter breakthrough caused by anomalous propagation.

4.6 BASE DATA SMOOTHING

Additional operations are applied to some of the "raw" base data fields prior to their utilization by the meteorological product generation algorithms. The DBDZ and DBV fields are median filtered over a window of nine nearest neighbor resolution cells before they are output to the meteorological product generation algorithms.

5. ALGORITHM IMPROVEMENT OPPORTUNITIES

There are several areas where the WSP signal processing algorithms could be enhanced to improve the quality of the data input to the meteorological product generation algorithms. These are under evaluation as candidate pre-planned product improvements (P^3I) for the WSP algorithm suite.

5.1 RECOVERY OF DEPOLARIZED SIGNAL ENERGY

In propagating long distances through heavy precipitation, circularly polarized (CP) radio waves may depolarize owing to differential phase delays for the horizontally and vertically polarized components. This would result in some of the precipitation echo energy returned to a radar having the same circular polarization sense as that transmitted (co-polarized). The WSP (like the existing ASR-9 six-level weather channel) only processes the cross-polarized receive path when the ASR-9 is in CP mode, thus raising the possibility of precipitation intensity underestimation, for example when the radar line of sight lies along a line of intense convective storms. We have observed possible instances of this effect in comparisons of ASR-9 weather channel data with other weather radars at our Laboratory's Integrated Terminal Weather System (ITWS) prototype sites. Figure 7 shows an example.

As noted the WSP has access to both cross- and co-polarized signals (the latter through the ASR-9 target channel A/D converters). Figure 8 is a modified version of the WSP signal processing overview shown previously (i.e. Figure 4) that includes a secondary processing channel to recover the co-polarized component of the echoes when the radar is in CP mode. If the energy in this co-polarized path significantly exceeded the system noise floor, the power returns from co- and cross-polarized signals would be summed to generate the reflectivity estimate.

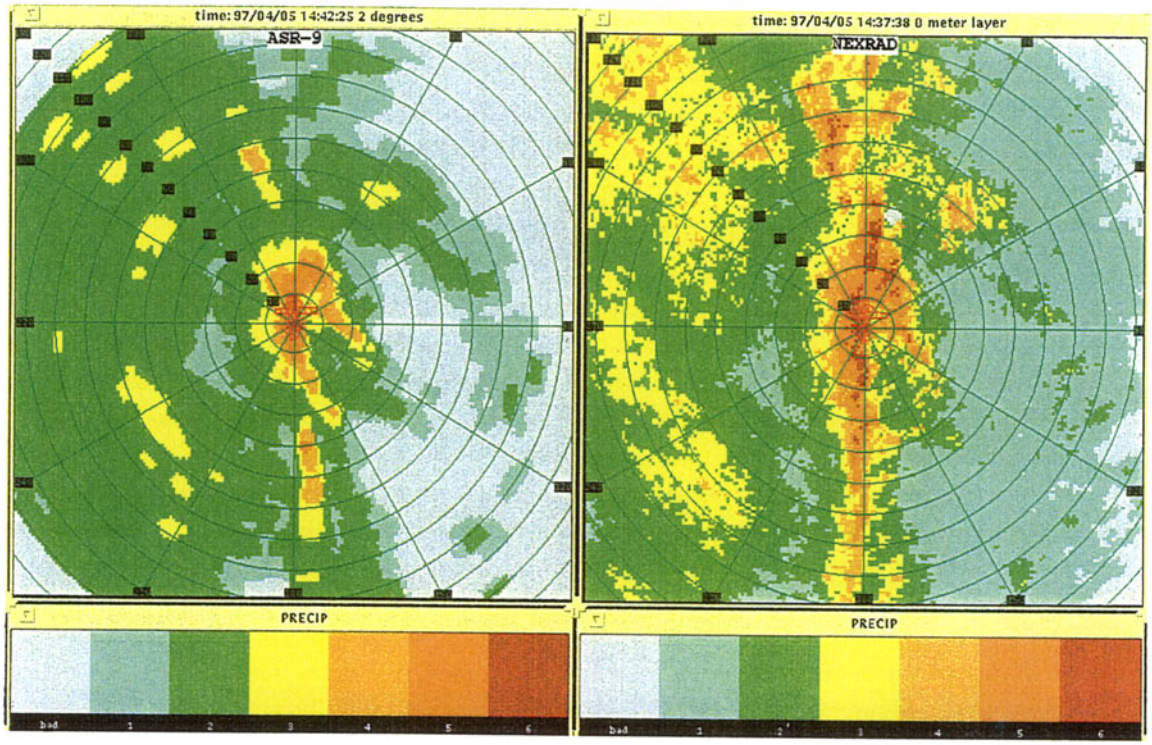

Figure 7. An example of possible ASR-9 signal loss due to depolarization of CP transmissions.

5.2 DOPPLER VELOCITY FOLDING

The ambiguous velocity associated with the ASR-9's long-PRI block may be as low as 24 m/s. Precipitation mean Doppler velocities may occasionally exceed this value even when measured through the vertically integrating beams of the ASR-9. The WSP "dual beam" velocity estimate used for microburst detection is formed from the phase-angle of a weighted subtraction of the low-and high-beam lag-one autocorrelation function (equation 14). When the component high and low beam vectors lie near the ambiguous limit, the result of this subtraction may lead to DBV aliasing even when the individual high or low beam inputs are less than their ambiguous velocities.

As described in the previous section, the WSP computes separately "partial" autocorrelation lags for the short- and long-PRI pulse blocks transmitted by the ASR-9. These may be manipulated to resolve Doppler ambiguities. A preliminary algorithm for accomplishing this has been worked out but has not to date been thoroughly tested or implemented in the WSP software suite.

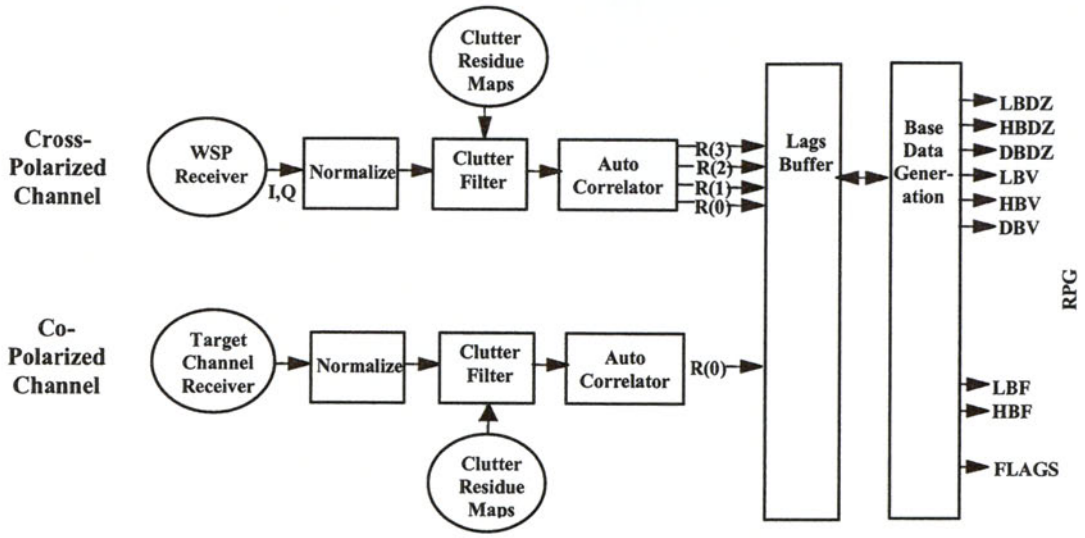

Figure 8. Parallel co- and cross-polarized channel processing to recover energy lost to signal depolarization.

5.3 OUT-OF-TRIP ANOMALOUS PROPAGATION DETECTION

The ASR-9 utilizes a "micro-stagger" to prevent range ambiguous ("out-of-trip") airplane returns in its target detection processor. For each successive pulse in a CPI, the pulse-repetition interval is increased by an amount equivalent to two range gates. Thus out-of-trip echoes will be split across multiple range gates and will not form a coherent return to the ASR-9 Doppler filter banks. This micro-stagger also decorrelates second trip ground clutter returns which may occur in the presence of strong ducting or anomalous propagation (AP) conditions. The WSP AP-detection test described in the previous section exploits the characteristics of the ground-clutter Doppler spectrum. It will not flag out-of-trip AP that is "whitened" owing to the ASR-9 microstagger. An example of out-of-trip AP breakthrough on the WSP "situation display" at Austin, TX is shown in Figure 9.

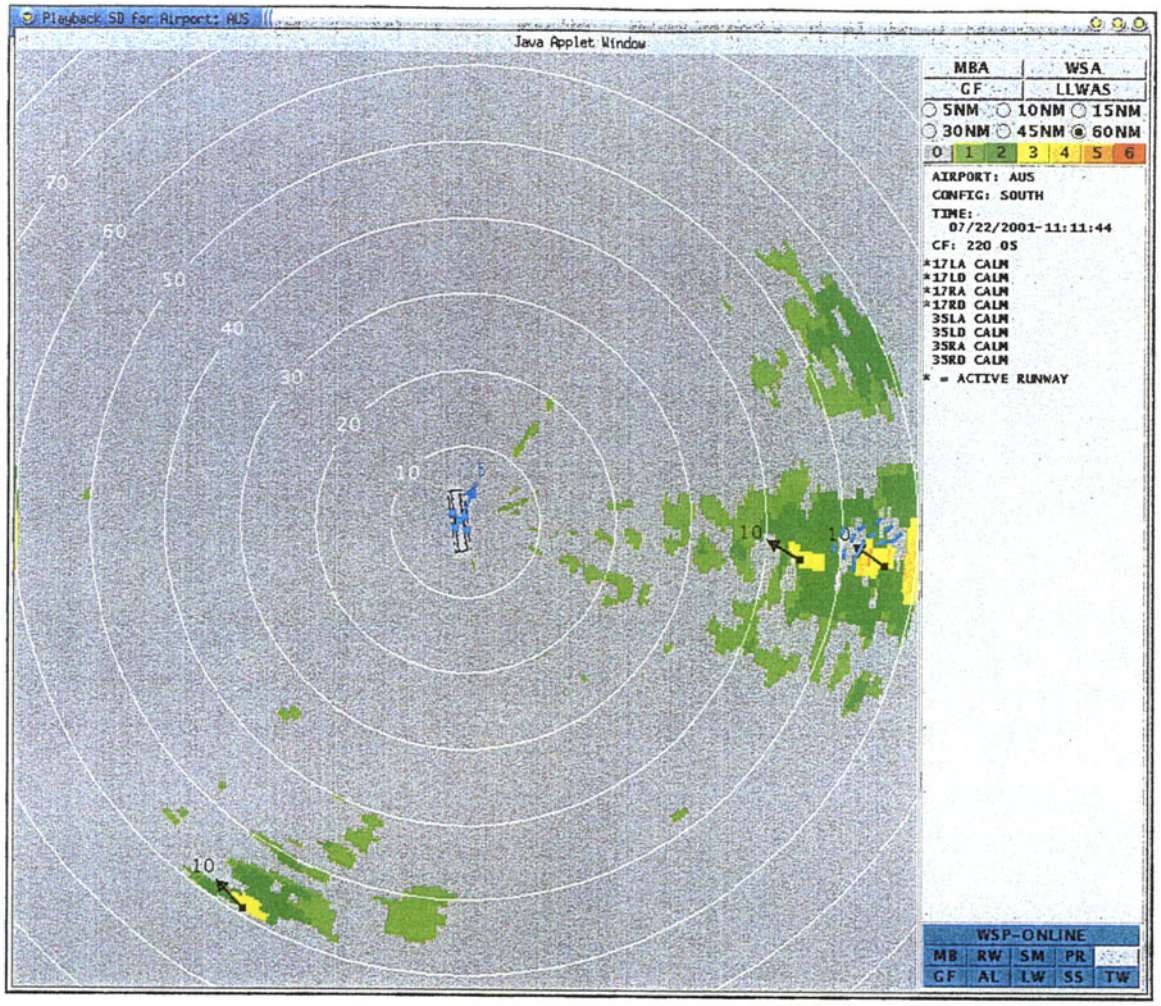

Figure 9. Out-of-trip ground clutter breakthrough caused by anomalous propagation at Austin, TX.

Note that the out-of-trip signal test described in the previous section may also fail to flag these returns as invalid. The large range extent of the AP ground clutter results in folding of returns from both long- and short-PRI blocks into the same range gates, thus confounding the differential power measurement upon which that test is based.

Out-of-trip returns could be recohered by realigning the pulse-returns across the WSP extended coherent processing interval to account for the microstagger. Resolution cells affected by coherent out-of-trip returns could be identified easily be computing the zeroth and first autocorrelation lags and taking their ratio. Values of R(1)/R(0) close to unity correspond to coherent returns and values near zero correspond to "white noise". A threshold applied to this ratio would identify resolution cells contaminated by range-

extensive out-of-trip returns (clutter or weather) and could be used to mitigate the observed AP breakthrough.

5.4 HIGH-ALTITUDE WEATHER DETECTION

Erroneous "dual-beam" (DBV) surface velocity estimates may occur in resolution cells where the precipitation reflectivity is concentrated well above the ground. This occurs, for example, on the edges of thunderstorm cells where strong winds aloft advect precipitation scatterers away from the storm core. In this circumstance, the dual-beam velocity estimate may erroneously reflect the winds at altitude. The WSP microburst detection algorithm employs various heuristics and a comparison of the low- and high-beam reflectivity estimates in an attempt to detect this occurrence and prevent associated microburst false detections.

More robust identification of resolution cells whose returns are dominated by scatterers at high elevation angle might be accomplished by computing and comparing the power spectrum density (PSD) of high and low beam signals. If the DBV estimate corresponded to an interval where the low beam PSD significantly exceeded that of the high beam, high confidence would be assigned to this estimate. (See Reference 3). Conversely, DBV estimates corresponding to intervals where the high beam PSD exceeds that of the low beam would be flagged as low confidence.

6. SUMMARY

This report has provided a functional overview of the ASR-9 WSP radar signal acquisition and processing subsystem with details of the digital processing operations required to generate base data images from radar quadrature samples. These algorithms have been tested extensively during WSP prototype and limited-production system operations at Albuquerque, NM; Austin, TX; and Norfolk, VA.

As noted in Section 5, ongoing algorithm enhancement and validation work may improve the quality of WSP base data. Owing to the WSP's open, expansible processor configuration and its use of readily modified, high-order language software, appropriate enhancements to these algorithms may readily be accomplished. Overall, however, the WSP's signal processing operations have been shown to reliably compensate for the non-standard configuration of the ASR-9 as a weather radar, in order to generate base data of sufficient quality to support robust performance of its meteorological detection algorithms.

APPENDIX A
WSP CLUTTER FILTERS

A.1 TRANSFER FUNCTIONS

Table A-1 defines the parameters of 12 high-pass filters to be used for ground clutter suppression in the ASR-9 Weather Systems Processor. From this set, three filters are selected for use at a particular site. These were designed using the multi-PRI filter design algorithm described by Chornoboy[6]. A C program implements this algorithm to provide Minimum Mean Squared Error (MMSE) high-pass filter matrices with user specified parameters. Only two of the program's design parameters – the filter stopband normalized width (SBFREQ), and the error tolerance for the stop-band notch (SBWT) – were varied in generating these filters. Settings for the remaining design parameters are listed in Table A-2.

TABLE A-1

Summary of WSP Clutter Filter Characteristics and Variable Design Parameters

Filter #	Clutter Suppression (dB)	6 dB Stopband Halfwidth (m/s)	Maximum Notch Depth (dB)	SBFREQ	SBWT
1	8.0	0.8	48	.007	5.0 e3
2	15.8	1.8	45	.010	5.0 e3
3*	20.4	2.3	42	.017	1.0 e4
4	25.7	2.7	55	.030	3.0 e4
5	30.6	3.0	65	.035	5.0 e4
6	35.9	3.4	60	.040	1.0 e5
7*	41.0	3.7	70	.047	2.0 e5
8	45.2	4.0	81	.045	1.0 e7
9	49.6	4.5	88	.050	1.5 e7
10	56.3	4.8	88	.055	2.0 e7
11*	61.2	5.0	91	.0625	4.0 e7
12	68.5	5.4	94	.071	6.5 e7

*Filters utilized in Lincoln Laboratory WSP prototypes

The clutter suppression calculation assumes a Gaussian clutter spectrum with width (0.72 m/s) consistent with antenna scan modulation. Clutter suppression and stopband halfwidth are calculated assuming PRF and transmitted frequency selections in the middle of the range allocated for the ASR-9. (The associated Nyquist velocities for the low and high-PRF CPI's are 25.3 and 32.5 m/s respectively.) As an example of the variation over the range of PRF and RF settings for the ASR-9, Filter 7 stopband halfwidth varies from 3.5 m/s (lowest PRF settings, highest transmitted frequency) to 4.2 m/s (highest PRF setting and lowest transmitted frequency). Clutter suppression for Filter 7 varies from 38.1 to 44.6 dB at these two extremes.

TABLE A-2

WSP Clutter Filter Design Parameters That Are Constant Across the Above Filter Set

Parameter	Value	Definition
LFREQ	SBFREQ-.0001	Normalized frequency for upper edge of negative Doppler passband
HFREQ	SBFREQ+.0001	Normalized frequency for lower edge of positive Doppler passband
PBWT	1.0	Error tolerance weight for passband magnitude response
PHWT	2.0	Error tolerance weight for passband phase response
MX_GAIN_WT	1.0	Constraint on filter gain
N_NYQ	2	Number of Nyguist intervals over which design optimization is attempted

Pulse-averaged magnitude and phase error responses are plotted in Figures A-1 and A-2. The abscissa is again calculated assuming mid-range values for ASR-9 transmitted frequency and PRF. The RMS phase error, quantifying the filters' departure from linear phase, is a measure of the Doppler error introduced by the filters. A value of 1/10 π for example (0.314), corresponds to an RMS Doppler velocity error of 1/10 of the Nyguist velocity – that is, 2.5 m/s – averaged across the 27 pulses that the filters operate on. In fact, the practical degradation on WSP Doppler velocity estimates will be much smaller because the phase error sign changes from pulse-to-pulse and across the band of Doppler velocities occupied by the weather signal.

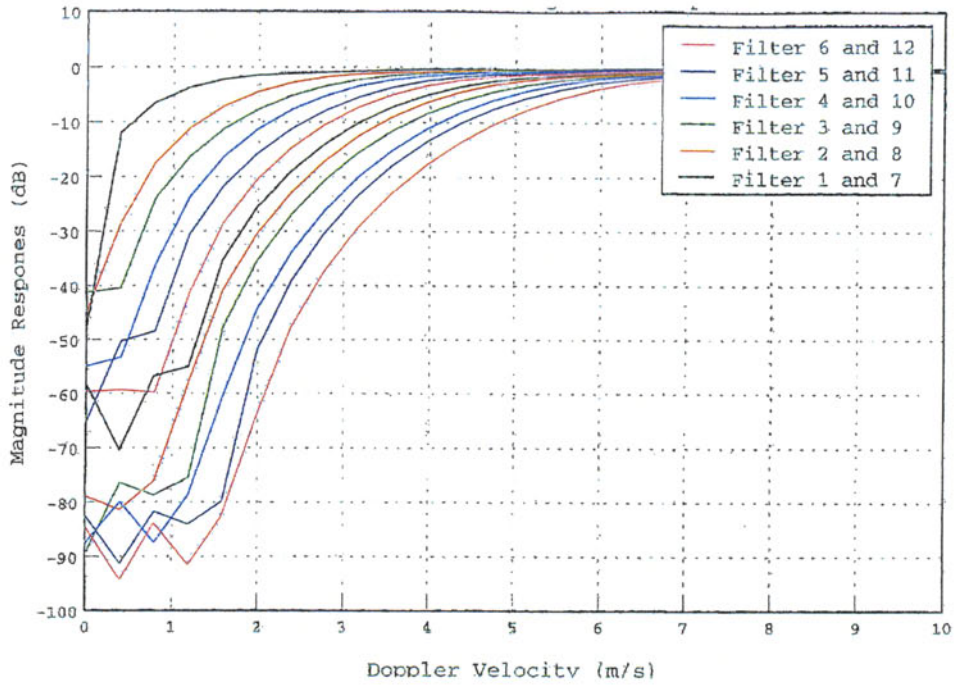

Figure A-1. WSP Clutter Filter Magnitude Responses

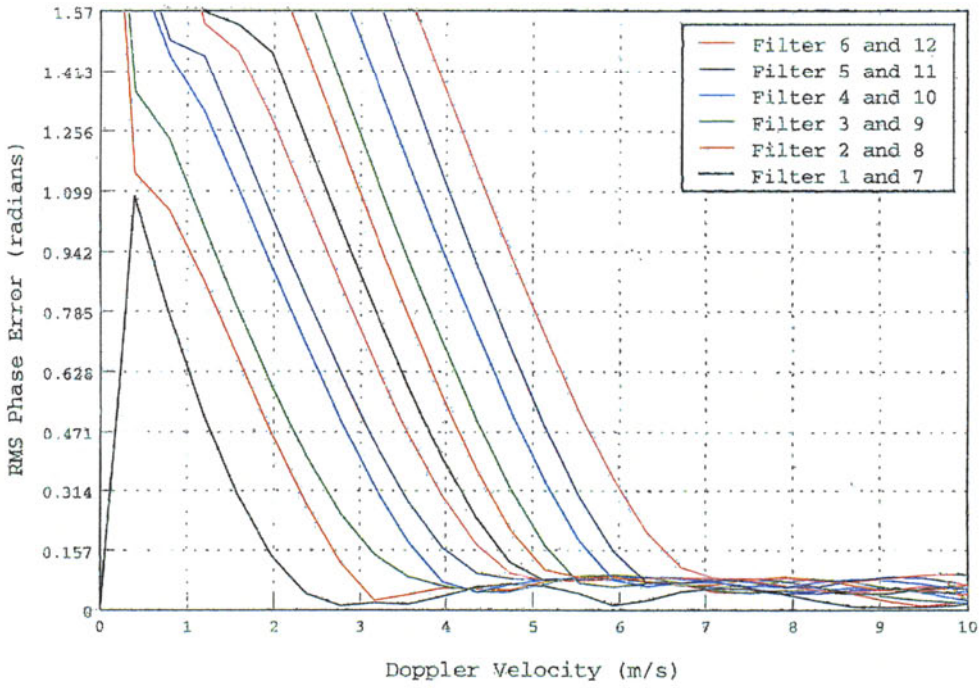

Figure A-2. WSP Clutter Filter Phase Error

A.2 METHODOLOGY FOR SELECTION OF PROCESSING SET

At any particular site, three of these filters (plus an all-pass function) are available for processing. This section defines an objective method for selecting the set of three high-pass filters for use at a specific WSP site based on the ground clutter intensity distribution and the expected distribution of wind shear reflectivity. The selected high-pass filters plus the all-pass filter are subsequently referred to as the "processing set".

Our selection method is based on the distribution of ground clutter reflectivity within the WSP wind shear detection range (0-15 nmi), and the distribution of reflectivity associated with the wind shear phenomena of concern. The former is to be obtained at each site as part of the WSP clutter map generation process. We recommend that the clutter distribution from the low-beam of the ASR-9 be used in selecting the filter processing set since the WSP wind shear detection algorithms rely primarily on low beam data. Wind shear reflectivity distributions will be estimated based on an understanding of the storm environment for the site. FAA-sponsored field measurement programs for Terminal Doppler Weather Radar (TDWR), WSP and Integrated Terminal Weather System (ITWS) provide an adequate database for defining wind shear reflectivity distributions in the major U.S. climatic regimes.

We denote the density functions for the clutter and wind shear reflectivity as $p(Z_c)$ and $p(Z_w)$. The probability that a given clutter filter will provide an output signal-to-clutter ratio (SCR) sufficient for Doppler velocity measurement is given by:

(1)

$$F_c = \int p(Z_c) \int_{Z_{c-s+T_1}}^{\infty} p(Z_w) dZ_w dZ_c$$

Here, S is the suppression realized by the clutter filter (given in Table 1), and T_1 is the required minimum SCR. We set T_1 equal to 11 dB as described in section 4.5.3.

The WSP signal-processing algorithms adaptively choose the least attenuating filter of the processing set that provides adequate SCR at its output. Given this approach, the frequency with which the different filters are invoked can be determined from the differences in F_c between the available filters. Specifically, if the filters in the processing set are denoted by "all-pass" "filt_1", "filt_2" and "filt_3", then their respective frequencies of usage are:

(2)

$$\begin{aligned}
&P(\text{all-pass}) = F_c(\text{all-pass}) \\
&P(\text{filt_1}) = F_c(\text{filt_1}) - F_c(\text{all-pass}) \\
&P(\text{filt_2}) = F_c(\text{filt_2}) - F_c(\text{filt_1}) \\
&P(\text{filt_3}) = F_c(\text{filt_3}) - F_c(\text{filt_2}) \\
&P(\text{censor}) = 1.0 - F_c(\text{filt_3})
\end{aligned}$$

Here, F_c (filt_n) denotes that equation (1) is to be evaluated using the clutter suppression associated with filt_n. The WSP sets a clutter censor flag when the most attenuating clutter filter cannot provide SCR in excess of T_1. The frequency with which this occurs is given by the last expression above.

We next assume that the "cost" associated with use of a particular filter is proportional to the size of the data-blind Doppler interval within its stop-band. Numerically, we set cost (filt_n) equal to the filter's stop-band width (again, given in Table 1) divided by the WSP Nyquist velocity of about 25 m/s. The aggregate cost for a given processing set (all-pass, filt_1, filt_2, filt_3) is:

$$\text{TOT\_COST} = P(\text{filt\_1})*\text{cost}(\text{filt\_1}) + P(\text{filt\_2})*\text{cost}(\text{filt\_2}) + P(\text{filt\_3})*\text{cost}(\text{filt\_3}) + P(\text{censor})*\text{cost}(\text{censor}) \quad (3)$$

We set the cost of a "censored" condition (i.e. SCR < T_0) equal to 0.5. This is about 4 times greater than the cost associated with use of the most attenuating filter defined in Table A-3.

The optimum set of high pass filters for a given environment is determined by evaluating equation 3 for all possible selections for "filt_1", "filt-2" and "filt_3" and choosing the processing set corresponding to the minimum value of "TOT_COST".

A.3 EXAMPLE CALCULATIONS

Figure A-3 shows clutter and wind shear density functions representative of the WSP prototype site in Albuquerque, NM. The clutter environment here is severe and "dry" wind shear phenomena occur frequently. The three components of the wind shear density distribution correspond to wet microbursts (centered at 48 dBz), dry microbursts (centered at 20 dBz) and gust fronts (centered at 10 dBz). Table A-3 summarizes the selected filter set.

TABLE A-3

Optimum WSP Clutter Filter Set for Environment Shown in Figure A-3

Filter #	Clutter Suppression (dB)	6 dB Stopband Halfwidth (m/s)	P (see Eq. 2)
0 (all-pass)	0	0	0.33
3 (filt_1)	20.4	2.3	0.27
7 (filt_2)	41.0	3.7	0.23
12 (filt_3)	68.5	5.4	0.15
censored			0.02

Figure A-4 illustrates the variation of the value for TOT_COST for the different processing sets. For display purposes, the x-axis value is an index incremented sequentially for each processing set that is evaluated. The order is:

(0,1,2,3), (0,1,2,4), …, (0,1,2,12), (0,1,3,4), …, (0,1,4,5), …, (0,1,11,12),

(0,2,3,4), (0,2,3,5), ……, (0,2,11,12),

(0,3,4,5), …., (0,3,11,12),

(0,4,5,6),……, (0,4,11,12),

……

(0,10,11,12)

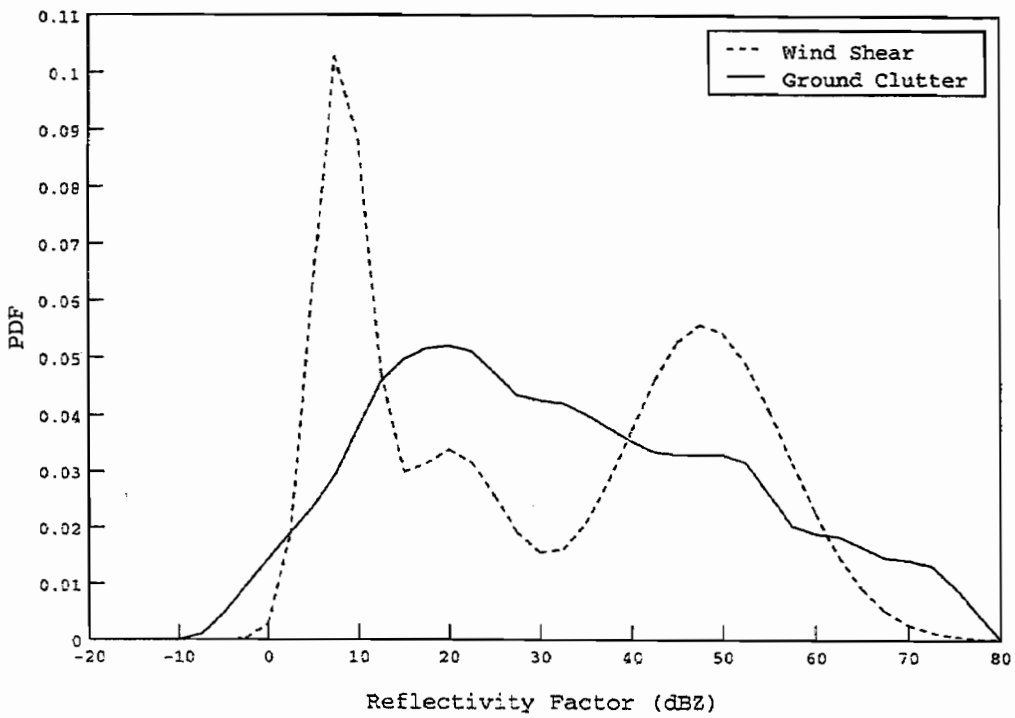

Figure A-3. Ground Clutter and Wind Shear Distribution (Albuquerque, NM).

The ten major groups across the plot correspond to constant values for filt_1. The generally descending segments within these groups have fixed values for filt_2.

The plot indicates that, for the defined clutter and wind shear reflectivity distributions, there are a number of processing sets that are near-optimum by our criterion. For example, sets (0,1,5,12), (0,2,7,12) and (0,4,8,12) as well as a number of others provide nearly equal values for TOT_COST.

A contrasting wind shear and clutter environment is shown in Figure A-5. Here, an exponential weight has been applied to the Albuquerque clutter reflectivity distribution so that the average clutter reflectivity is significantly lower. The wind shear reflectivity distribution is dominated by wet microbursts centered around 50 dBZ; gust fronts constitute a second component centered at 15 dBZ. The optimum clutter filter set (Table A-5) involves less attenuating filters than those definined for the previously considered environment, and the selected high-pass filters are used less frequently. As shown in Figure A-6, there are again a number of processing sets that provide nearly equal values for TOT_COST. The near optimum sets, however, involve generally less attenuating filters than those for the environment defined in Figure A-3.

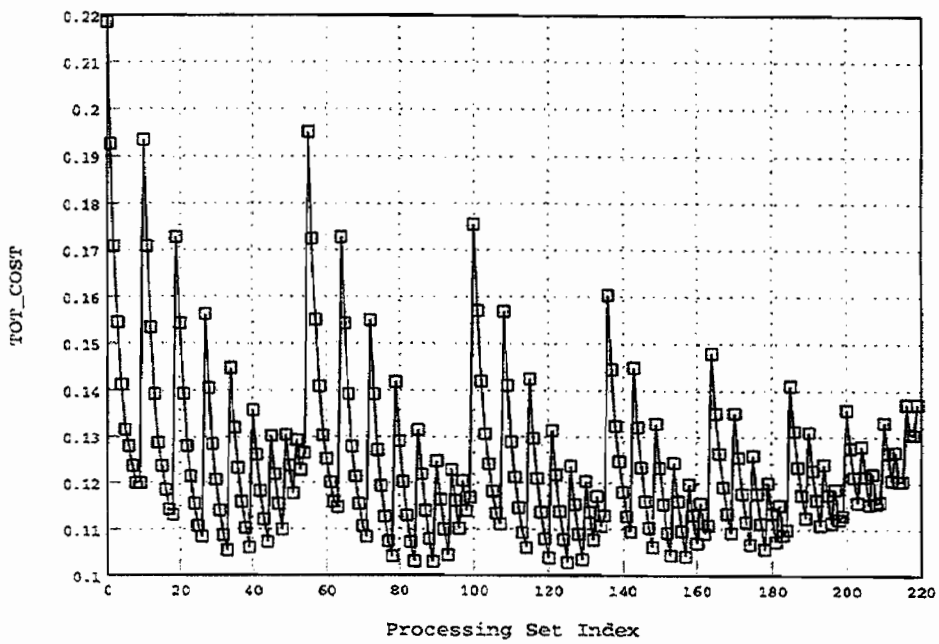

Figure A-4. Cost versus Clutter Filter Set (ABQ, NM).

TABLE A-4

Optimum WSP Clutter Filter Set for Environment Shown in Figure A-5

Filter #	Clutter Suppression (dB)	6 dB Stopband Halfwidth (m/s)	P (see Eq. 2)
0 (all-pass)	0	0	0.64
2 (filt_1)	15.8	1.8	0.18
5 (filt_2)	30.6	3.0	0.11
12 (filt_3)	68.5	5.4	0.07
censored			0.002

A.4 COMMENTS AND RECOMMENDATIONS

This methodology can provide guidance for selecting the clutter filter processing set as part of the WSP site optimization process. As indicated, there will generally be a number of near optimum processing sets available and it may be appropriate to deviate from the set with absolute minimum TOT_COST in some circumstances. For example, the actual clutter suppression realized by a particular filter may differ from the design value owing to:

1. radar imperfections (i.e. transmit and receive chain stability limitations);
2. receiver noise which sets a limit on how far a clutter signal may be suppressed;
3. clutter spectrum broadening (moving ground targets).

As a result, the higher number filters will generally provide significantly less suppression on average than indicated in Table A-1. This consideration suggests that use of a slightly narrower stop-band for filt_3 (e.g. filter 10 or 11 instead of filter 12) may reduce the potential distortion of weather echoes without a measurable increase in the clutter residue.

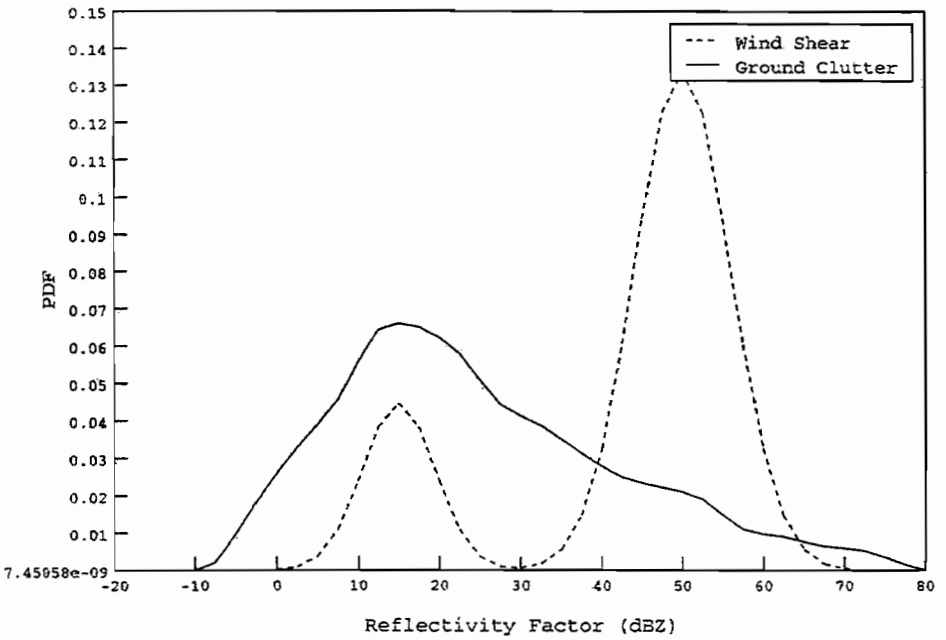

Figure A-5. Ground Clutter and Wind Shear Distributions (Benign Environment)

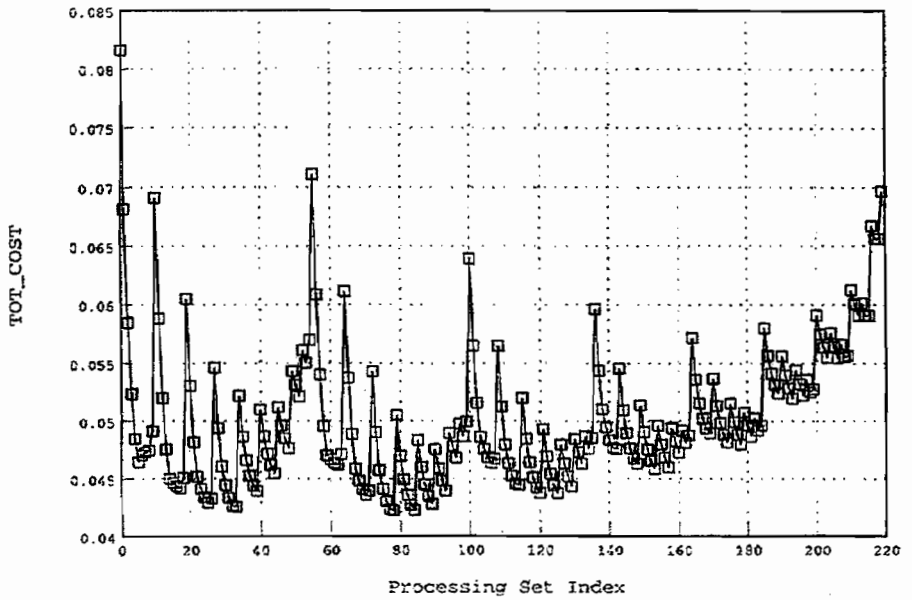

Figure A-6. Cost versus Clutter Filter Set (Benign Environment)

GLOSSARY

A/D	Analog-to-Digital
ACP	Azimuth Control Pulse
ARP	Airport Reference Point
ASR-9	Airport Surveillance Radar
CDM	Clutter Day Map
CP	circularly polarized
CPI	Coherent Processing Interval
CRM	Clutter Residue Maps
DBDZ	Dual Beam Reflectivity
DBV	Dual-Beam Velocity
ECPI	Extended Coherent Processing Interval
FAA	Federal Aviation Administration
FIR	Finite Impulse Response
FSD	Full-scale Development
GFE	Government Furnished Equipment
HBDZ	High-Beam Reflectivity
HBV	High-Beam Velocity
LBDZ	Low Beam Reflectivity
LBV	Low-Beam Velocity
LLWAS	Low Level Wind Shear Alert System
LP	linearly polarized
MBYTES	million bytes
PRF	Pulse Repetition Frequency
PRI	Pulse Repetition Interval
RAG	Range-Azimuth Gated
RMS	Remote Monitoring System
STC	Sensitivity Time Control
TDWR	Terminal Doppler Weather Radar
VSPs	Variable Site Parameters
WSP	Weather Systems Processor

REFERENCES

1. M.E. Weber, R.L. Delanoy, and E.S. Chornoboy, "Data Processing Techniques for Airport Surveillance Radar Weather Sensing," IEEE National Radar Conference, March 1995.

2. M.E. Weber, "Ground Clutter Processing for Wind Measurements with Airport Surveillance Radars," MIT Lincoln Laboratory, Lexington, MA, Project Report ATC-143, 4 November 1987.

3. M.E. Weber, "Dual-Beam Autocorrelation Based Wind Measurements from Airport Surveillance Radar Signals," MIT Lincoln Laboratory, Lexington, MA, Project Report ATC-167, 21 June 1989.

4. M.L. Stone, J.J. Saia and M.E. Weber, "A Description of the Interfaces between the Weather Systems Processor (WSP) and the Airport Surveillance Radar (ASR-9)," MIT Lincoln Laboratory, Lexington, MA, Project Report ATC-259, 6 June 1997.

5. D. Doviak and D. Zrnic, Doppler Weather Radar (book, c. 1984).

6. E.S. Chornoboy, "Clutter Filter Design for Multiple-PRT Signals," 26th Conference on Radar Meteorology, Norman, OK, May 1993.